Available online at www.sciencedirect.com
ScienceDirect
Colloids and Surfaces A: Physicochem. Eng. Aspects 317 (2008) 366–376
COLLOIDS AND SURFACES A
www.elsevier.com/locate/colsurfa

Photocatalytic activity of nanocrystalline TiO_2 (brookite, rutile and brookite-based) powders prepared by thermohydrolysis of $TiCl_4$ in aqueous chloride solutions

Agatino Di Paola [a,*], Giovanni Cufalo [a], Maurizio Addamo [a], Marianna Bellardita [a], Renzo Campostrini [b], Marco Ischia [b], Riccardo Ceccato [b], Leonardo Palmisano [a]

[a] *Dipartimento di Ingegneria Chimica dei Processi e dei Materiali, Università di Palermo, Viale delle Scienze, 90128 Palermo, Italy*
[b] *Dipartimento di Ingegneria dei Materiali e delle Tecnologie Industriali, Via Mesiano 77, 38050 Trento, Italy*

Received 11 June 2007; received in revised form 4 October 2007; accepted 6 November 2007
Available online 13 November 2007

Abstract

Nanocrystalline TiO_2 powders were synthesized by thermohydrolysis of $TiCl_4$ in HCl or NaCl aqueous solutions. Rutile, mixtures of brookite and rutile or mixtures of anatase, brookite and rutile were obtained depending on the acidity of the medium. Crystalline phases and composition of the mixtures were identified by using XRD analysis. Pure brookite nanoparticles, separated from the mixtures of brookite and rutile by simple peptization with water, were stable against transformation to rutile up to 750 °C. The prepared TiO_2 powders were characterized by thermal analysis, diffuse reflectance spectroscopy and BET surface area determinations. The band gap of bulky brookite was estimated 3.29 eV. 4-Nitrophenol photodegradation was used to evaluate the photocatalytic activity of the various samples. The highest activity corresponded to the powders consisting of more than one crystalline phase.

Keywords: Anatase; Brookite; Rutile; Mixed phase TiO_2; Brookite band gap; Photocatalyst

1. Introduction

Heterogeneous photocatalysis is an attractive approach for the destruction of inorganic and organic pollutants present in air and water [1]. Among various semiconductors, TiO_2 is the most used photocatalyst because of its high efficiency, nontoxicity, chemical and biological stability, and low cost. TiO_2 exists in three different crystalline habits: rutile (tetragonal), anatase (tetragonal) and brookite (orthorombic). All three crystalline structures consist of deformed TiO_6 octahedra connected differently by corners and edges. In rutile, two octahedra edges are shared to form linear chains along the [0 0 1] direction and the TiO_6 chains are linked to each other through corner-shared bondings. In anatase, each octahedron shares four edges with other four octahedra, resulting in a zigzag structure. In brookite, each octahedron shares three edges and the octahedra arrangement produces a crystalline structure with tunnels along the *c*-axis.

Rutile is the stable form, whereas anatase and brookite are metastable and are readily transformed to rutile when heated. Anatase is the phase normally found in the sol–gel syntheses of TiO_2 but brookite is often observed as a by-product when the precipitation is carried out in an acidic medium at low temperature. Pure brookite without rutile or anatase is rather difficult to be prepared.

Brookite has been prevalently obtained from titanium (IV) compounds in aqueous or organic media via hydrothermal treatment at high temperatures. Highly crystalline brookite was prepared by Keesmann [2] by hydrolysis of Ti isopropoxide with water, in the presence of NaOH. Mitsuhashi and Watanabe [3] crystallized the brookite form by hydrothermal treatment at 220–560 °C of the precipitate prepared from an aqueous solution of $TiCl_4$ and $CaCl_2$. Nagase et al. [4] prepared brookite as almost single-phase from amorphous TiO_2 in NaOH solution at 200 °C. Kominami et al. synthesized microcrystalline brookite by solvothermal treatment of

* Corresponding author. Tel.: +39 091 6567229; fax: +39 091 6567280.
E-mail address: dipaola@dicpm.unipa.it (A. Di Paola).

0927-7757/$ – see front matter © 2007 Elsevier B.V. All rights reserved.
doi:10.1016/j.colsurfa.2007.11.005

oxobis(2,4-pentanedionato-O,O′)titanium in ethylene glycol in the presence of sodium laurate [5] or sodium acetate [6,7] and a small amount of water in an autoclave at 300 °C. Zheng et al. [8] prepared brookite powders by hydrothermal treatment of basic solutions of $Ti(SO_4)_2$ or $TiCl_4$. Polycrystalline brookite-type ultrafine powders were obtained by hydrolyzing titanium sulphate in alkaline medium at 199 °C [9]. Tomita et al. [10] synthesized nanopowders of single-phase brookite by hydrothermal treatment of a water-soluble titanium complex prepared from titanium powder, H_2O_2, NH_3(aq.) and glycolic acid, at 200 °C and pH 10.

Pure brookite particles were also obtained by selective peptization with HNO_3 of mixtures of rutile and brookite prepared by thermolysis of $TiCl_4$ in HCl media [11]: the relative proportions of the two phases were dependent on acidity, titanium concentration, temperature and reaction time [11–13]. Recently, brookite nanoparticles were prepared at low temperature by hydrolysis of $TiCl_4$ using HNO_3 solutions [14] or in an acidic isopropyl solution under refluxing [15].

Titanium (III) compounds have been rarely used for the synthesis of brookite. Ohtani et al. [16] prepared extra-fine crystallites of brookite by air oxidation of $TiCl_3$ in aqueous HCl solution, in the presence of sodium acetate. Li et al. [17,18] synthesized brookite nanocrystals under ambient pressure at 70 °C by reaction of a mixed solution of urea and $TiCl_3$. Nanometric particles of pure brookite were obtained by modified thermolysis of reactant solutions containing $TiCl_3$ prepared from titania powder and concentrated HCl, urea and PEG 10000 [19].

A brookite sol for thin film coating was prepared by hydrothermal treatment of a Ti peroxo solution obtained by dissolving Ti hydroxide in hydrogen peroxide [20]. Brookite films were deposited by stable sols of pure brookite prepared by thermolysis of $TiCl_4$ in diluted HCl solutions [21–23]. A pure brookite film with a preferred orientation was obtained by Kutnetsova et al. [24] by a spin-coating method from a solution of $TiCl_4$ in ethanol with cellulose and oxalic acid as complexing agent.

Many papers have concerned the photocatalytic application of TiO_2 and it is generally accepted that anatase is more efficient as photocatalyst than rutile and brookite [1]. Rutile has been found rarely active for the photodegradation of organic species in aqueous solutions [25,26] but a good photoactivity has been shown by samples containing anatase, brookite and rutile [19,27]. Only few studies have examined the photocatalytic activity of pure brookite TiO_2 powders or films. Ohtani et al. [16] found that brookite nanocrystals possessed good photocatalytic capacities for silver deposition and dehydrogenation of 2-propanol. Microcrystalline brookite powders, prepared by solvothermal technique, exhibited higher or similar photoactivities than commercial photocatalysts for the mineralization of acetic acid and dehydrogenation of 2-propanol [7,8]. Nanocrystalline brookite particles obtained by reaction of $TiCl_3$ and urea revealed a good efficiency for the photodegradation of acetaldehyde [17] and 4-chlorophenol [19]. Thin films of brookite showed a good efficiency for the gas-phase photooxidation of 2-propanol [22,23].

In this study, pure rutile or binary mixtures of brookite and rutile or ternary mixtures of anatase, brookite and rutile, were obtained by thermolysis of $TiCl_4$ in aqueous chloride solutions. Brookite was separated from rutile by peptization with water. The reactivity of all samples, both pure phases and mixtures, was tested for the photocatalytic degradation of 4-nitrophenol (4-NP), and compared to that of a commercially available TiO_2 material.

2. Experimental

2.1. Synthesis

Titanium tetrachloride (98% Fluka) was used as the starting material without further purification. Three different routes were followed to synthesize the various samples: hydrolysis in diluted HCl solutions, hydrolysis in concentrated HCl, hydrolysis in NaCl solutions. HCl (37 wt%, $d = 1.19\ g\ cm^{-3}$) pure reagent grade (Backer) and NaCl RPE (Carlo Erba Reagents) were used. The syntheses were carried out in Pyrex bottles or flasks previously cleaned with aqua regia and demineralized water.

2.1.1. Hydrolysis in diluted HCl solutions

$TiCl_4$ was added dropwise under stirring to aqueous HCl solutions, at room temperature. The concentration of the acid was varied between 1.43 and 5.12 mol dm^{-3} ($TiCl_4$/HCl/H_2O volume (cm^3) ratios 1/7/41, 1/10/48, 1/16/42 and 1/25/33 corresponding to molar [Cl]/[Ti] ratios equal to 13, 18, 26 and 38, respectively). The hydrolysis reaction was highly exothermic and released fumes of HCl. The dispersions produced by this treatment were the more opalescent the less the acid concentration. Clear transparent solutions were obtained after continuous stirring for times ranging between 15 min and 4 h, depending on the acidity of the medium.

The solutions were heated in closed bottles and aged at 100 °C in an oven, or alternatively, allowed to boil with constant stirring in a standard reflux apparatus. Rutile or various mixtures of the three polymorph TiO_2 phases were obtained. Pure brookite nanoparticles were separated by peptization from the binary mixtures of brookite and rutile by removing many times the supernatant and adding water to restore the initial solution volume. When the pH was higher than 0.8, a dispersion of brookite particles formed while the rutile phase remained as precipitate. The dispersion was recovered and the treatment was repeated till a transparent liquid covered the solid rutile. The sol containing the brookite particles and the precipitate of rutile were separately dried under vacuum at 55 °C.

2.1.2. Hydrolysis in concentrated HCl

$TiCl_4$ was added dropwise under stirring to concentrated HCl ($TiCl_4$/HCl volume (cm^3) ratios 1/10, 1/16 and 1/25 corresponding to molar [Cl]/[Ti] ratios equal to 18, 26 and 38, respectively) at room temperature. Clear yellow solutions were obtained due probably to the formation of $TiOCl_2$ [28]. After heating under reflux for 24 or 48 h white precipitates of rutile were formed. The flasks were allowed to cool to room temperature, the

supernatant liquid was removed and the solid was dried under vacuum at 55 °C.

2.1.3. Hydrolysis in NaCl solutions

Five cm^3 of $TiCl_4$ (4.56×10^{-2} mol) were added dropwise to 200 or 500 cm^3 of aqueous NaCl solutions (corresponding to molar $[Cl]_{total}/[Ti]$ ratios equal to 18, 26 and 38, respectively). The final chloride concentration was varied between 3.34 and 5.58 mol dm^{-3}.

The solutions were heated and aged at 100 °C in the oven, or boiled with constant stirring under reflux. The reaction mixtures were allowed to cool to room temperature and were dialyzed (Dialysis tubing cellulose membrane with MW 12400 cut off pores) against 4 dm^3 of water (replaced every day) in order to eliminate the large amount of NaCl. The final pH of the suspension depended on the length of dialysis and the concentration of TiO_2. After removal of the supernatant liquid, the solid was dried under vacuum at 55 °C.

2.2. Characterization of the samples

2.2.1. X-ray diffraction

X-ray diffraction spectra of the powders were recorded at room temperature using a powder diffractometer (Rigaku D-max) employing the CuK_α radiation ($\lambda = 0.154056$ nm) and a graphite monochromator in the diffracted beam. Typical scans were performed in the 2θ 20–60° range, with a sampling range of 0.05° and 6 s counting time. Quantitative analyses of the samples were performed using a modified Rietveld method, developed for the determination of amorphous and crystalline phases in ceramic materials [29]. This method allows the determination of the crystallite sizes on the basis of the Warren–Averbach theory [30].

2.2.2. Diffuse reflectance spectroscopy

Visible–ultraviolet spectra were obtained by diffuse reflectance spectroscopy by using a Shimadzu UV-2401 PC instrument. $BaSO_4$ was the reference sample and the spectra were recorded in the range 200–800 nm.

2.2.3. Specific surface area and porosity

Nitrogen physisorption experiments were performed at the liquid nitrogen temperature using a Micromeritics ASAP 2010 system. All the samples were degassed below 1.3 Pa at 250 °C prior to the measurement. The specific surface area (SSA) values were calculated by the BET equation in the interval $0.05 \leq (p/p_o) \leq 0.33$. Pore size distribution was calculated using the BJH method applied on the adsorption branch of the isotherms.

2.2.4. Thermoanalysis

Thermogravimetric (TG) and differential thermal analyses (DTA) were performed on a LabSys Setaram thermobalance. Thermal analyses were carried out in the range 20–1000 °C, with a heating rate of 10 °C min^{-1}, by working under 200 cm^3 min^{-1} He flow. Powdered samples (20–40 mg) were analysed in 0.1 cm^3 alumina crucible by using α-Al_2O_3 as reference. Any species released in gas-phase from the solid sample during the thermogravimetric analysis was directly transferred and detected by a mass spectrometer by means of an appropriate transfer line. This was lab-assembled by using a deactivated silica capillary column [31]. The mass spectra analyses were carried out by using VG-QMD-1000 Carlo Erba Instruments quadrupole mass spectrometer. Electron impact mass spectra (70 eV) were continuously recorded with frequency 1 scan s^{-1} in the 3–500 amu range.

2.3. Photoreactivity measurements

A Pyrex batch photoreactor of cylindrical shape containing 0.5 dm^3 of aqueous suspension was used. The photoreactor was provided with ports in its upper section for the inlet and outlet of gases, for sampling and for pH and temperature measurements. A 125 W medium pressure Hg lamp (Helios Italquartz, Italy) was immersed within the photoreactor. The photon flux emitted by the lamp was $\Phi_i = 13.5$ mW cm^{-2}: it was measured by using a radiometer "UVX Digital" leaned against the external wall of the photoreactor containing only pure water. O_2 was continuously bubbled into the suspensions for ca. 0.5 h before switching on the lamp and throughout the occurrence of the photoreactivity experiments. The temperature inside the reactor was ca. 30 °C.

The amount of catalyst was 0.6 g dm^{-3} and the initial 4-nitrophenol (BDH) concentration was 20 g dm^{-3}. The initial pH of the suspensions was always in the range 3–3.5. Samples of 5 cm^3 volume were withdrawn from the suspensions every 5, 30, or 60 min and the catalyst was separated from the solution by filtration through 0.1 μm Teflon membranes (Whatman). The quantitative determination of 4-nitrophenol was performed by measuring its absorption at 315 nm with a spectrophotometer Shimadzu UV-2401 PC.

3. Results

3.1. Characterization

Pure anatase, brookite, and rutile or mixture of the TiO_2 polymorphs can be prepared by thermolysis of $TiCl_4$ in different mineral acids [11,14]. The existence of brookite in XRD patterns is clearly evidenced from the presence of the (1 2 1) peak at $2\theta = 30.81°$. Anyway, for the interpretation of the diffractograms it is necessary to take into account that the main (1 0 1) diffraction peak of anatase at $2\theta = 25.28°$ overlaps with the (1 2 0) and (1 1 1) peaks of brookite at $2\theta = 25.34°$ and 25.69°, respectively. So, as underlined by Bokhimi and Pedraza [32], apparently pure brookite samples can be a mixture of anatase and brookite. A numerical deconvolution technique [31] was used to separate overlapping XRD peaks in order to determine the relative proportions of the different TiO_2 phases present in the solids. Quantitative analyses of the samples were carried out considering PDF cards related to pure phases of the titanium dioxide polymorphs: anatase (21–1272), rutile (21–1276) and brookite (29–1360).

Mixtures of brookite and rutile were prevalently obtained when the hydrolysis of $TiCl_4$ occurred in diluted HCl. Small

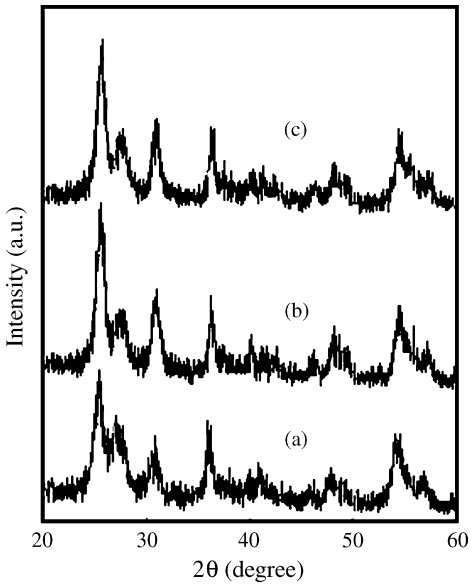

Fig. 1. XRD patterns of the solids obtained by thermolysis of a solution of $TiCl_4$ (0.15 mol dm^{-3}) in diluted HCl ([Cl]/[Ti] = 18) under reflux for different times. (a) 12 h; (b) 48 h; (c) 72 h.

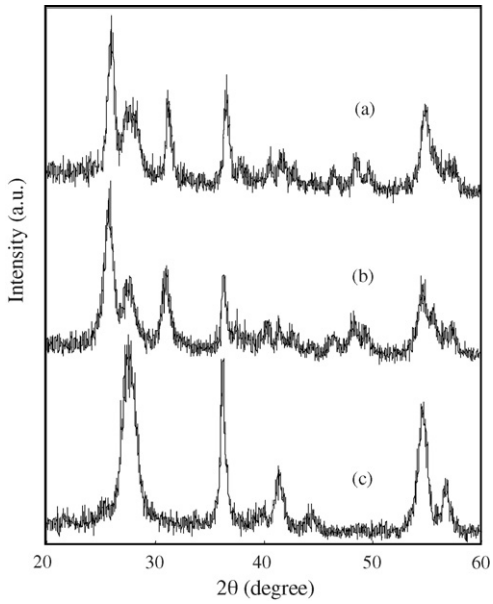

Fig. 3. XRD patterns of the solids obtained by thermolysis of solutions of $TiCl_4$ (0.15 mol dm^{-3}) in diluted HCl with different [Cl]/[Ti] ratios under reflux for 48 h. (a) [Cl]/[Ti] = 18; (b) [Cl]/[Ti] = 26; (c) [Cl]/[Ti] = 38.

amounts of anatase were always present in the early stages of precipitation but disappeared after long heating times ($t > 48$ h). Fig. 1 reports XRD patterns of the solids formed by thermolysing a $TiCl_4$ solution with a [Cl]/[Ti] = 18, for different reaction times. The variation of the relative proportions of the three TiO_2 phases as a function of the heating time is shown in Fig. 2: anatase progressively disappeared, rutile diminished and brookite increased. Similar results were obtained if the solutions were boiled under reflux or heated at 100 °C in the oven.

The composition of the TiO_2 powders depended on the acidity of the medium and the concentration of titanium [11–13]. As shown in Fig. 3 the increase of the [Cl]/[Ti] ratio and the corresponding pH reduction favored the formation of rutile. Table 1 reports the concentrations in wt% of anatase, brookite and rutile present in various samples after 48 h of thermolysis under different experimental conditions. For [Ti] = 0.15 mol dm^{-3}, brookite and rutile were prevalently formed if the [Cl]/[Ti] ratios were 18 and 26, whereas a ternary mixture of anatase, brookite and rutile was obtained if [Cl]/[Ti] = 13.5. In the presence of a low $TiCl_4$ concentration ([Ti] = 0.06 mol dm^{-3}) brookite and rutile precipitated even when the [Cl]/[Ti] ratio was high.

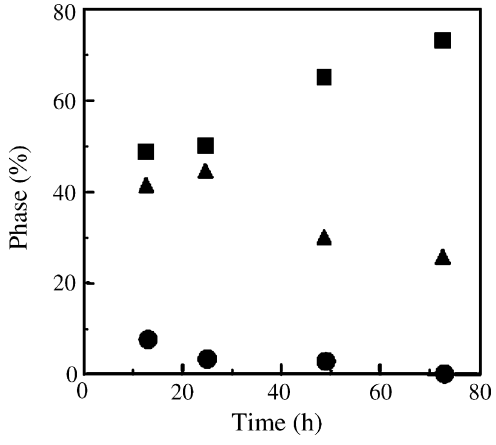

Fig. 2. Change of the relative proportions of (●) anatase, (■) brookite and (▲) rutile with heating time. The solids were obtained by thermolysis of a solution of $TiCl_4$ (0.15 mol dm^{-3}) in diluted HCl ([Cl]/[Ti] = 18).

Fig. 4b shows the XRD pattern of the powder obtained by drying a precipitate containing a mixture of brookite and rutile. Fig. 4(a and c) confirm that the solids separated after selective peptization contained only single-phase rutile or brookite. The identity of the two TiO_2 polymorphs was also verified by Raman spectroscopy. As reported in a previous work [22], all peaks of the Raman spectrum of the as-prepared brookite powder were consistent with those of natural brookite crystals.

As shown in Table 2, the crystallite dimensions evaluated from the line profile analysis of the XRD peaks [30] indicated that all as-prepared samples were nanocrystalline and the mean diameter of the crystallites was lower than 10 nm.

Fig. 5 shows the diffuse reflectance spectra of brookite, rutile and of a mixture of the two phases. TiO_2 is an indirect semiconductor [33] so that the band gap energy, E_g, of the samples can be determined from the tangent lines to the plots of the modified Kubelka-Munk function, $[F(R'_\infty)h\nu]^{1/2}$, versus the energy of the exciting light [34]. As shown in the inset of Fig. 5, the E_g values of rutile and brookite were 2.95 and 3.25 eV, respectively. The band gap of rutile is very close to that determined for a pure commercial rutile sample (provided by Tioxide Huntsman) whereas the E_g of brookite is in good agreement with data found in the literature [21,35,36]. The spectrum of the mixture of brookite and rutile revealed two threshold wavelengths indicative of the contemporaneous presence of the different TiO_2 phases. The E_g values of various powders are reported in Table 2. The increased band gap exhibited by the samples calcined at

Table 1
Crystal phase composition of TiO_2 powders prepared under different experimental conditions

Thermolysis conditions[a]		[Ti] (mol dm^{-3})	[Cl]/[Ti]	Anatase %	Brookite %	Rutile %
Under reflux	Diluted HCl	0.15	18	3.5	65.8	30.7
Under reflux	Diluted HCl	0.15	26		50.3	49.7
Under reflux	Diluted HCl	0.15	38			100
Under reflux	Diluted HCl	0.06	38		39.5	60.5
Oven	Diluted HCl	0.15	13.5	20.3	60.3	19.4
Oven	Diluted HCl	0.15	18		55.4	44.6
Oven	Diluted HCl	0.15	26		56.5	43.5
Oven	Diluted HCl	0.15	38			100
Under reflux	Concentrated HCl	0.15	18			100
Under reflux	Concentrated HCl	0.15	26			100
Under reflux	Concentrated HCl	0.15	38			100
Oven	NaCl	0.22	18	29.7	6.9	63.4
Oven	NaCl	0.22	26	5.0	6.3	88.7
Oven	NaCl	0.09	38	66.0	24.9	9.1

[a] All samples were heated for 48 h.

high temperatures is attributable to a better crystallization of the solids. The band gaps of the mixtures of two or three phases were lower than those of anatase and brookite.

Fig. 6 shows the diffractograms of the solids obtained after thermal treatment of pure brookite for 2 h at different temperatures. At 450 °C the peaks of brookite increased without change of the crystal structure. At 750 °C the XRD pattern clearly revealed the presence of the two distinct peaks of brookite at 25.40° and 25.72°, respectively. At 800 °C the peak intensities of brookite decreased and new large peaks corresponding to rutile appeared. At 900 °C only peaks of rutile were observed indicating that brookite was completely transformed to rutile.

The thermal analyses of the pure brookite sample are reported in Fig. 7. The TG curve revealed a continuous mass loss from 75

Table 2
Crystallite size (Φ), specific surface area (SSA), initial reaction rate (r_o) and band gap (E_g) of TiO_2 powders prepared by various routes

Phase	Composition (wt%)	Hydrolysis solution	Φ (nm)	SSA (m^2 g^{-1})	$r_o \times 10^9$ (mol dm^{-3} s^{-1})[a]	E_g (eV)
Rutile	100	dil. HCl	3.8	24	9.9	2.95
Rutile	100	conc. HCl	4.3	29	12.5	2.98
Rutile[b]	100	conc. HCl	25.4	2	3.2	2.95
Rutile Tioxide	100	conc. HCl	50	8	negligible	3.02
Brookite	100	dil. HCl	6.6	82	14.9	3.25
Brookite[c]	100	dil. HCl	7.5	69	16.4	3.28
Brookite[d]	100	dil. HCl	9.7	46	23.6	3.29
Brookite[e]	100	dil. HCl	16.4	18	18.4	3.24
Rutile[f]	100	dil. HCl	32.7	12	7.8	2.95
Brookite	73.6	dil.	4.3	141	16.5	3.15
Rutile	26.4	HCl	4.2			3.00
Brookite	39.5	dil.	9.0	35	11.2	3.16
Rutile	60.5	HCl	4.7			2.96
Anatase	70.9		2.2	189	21.6	3.00
Brookite	16.2	NaCl	2.7			
Rutile	12.9		7.1			
Anatase	29.7		2.7	138	14.3	3.02
Brookite	6.9	NaCl	5.4			
Rutile	63.4		5.0			
P25						
Anatase	80		25.1	50	43.0[g]	3.02
Rutile	20		33.2			

[a] All the runs were carried out at pH 3.3.
[b] As-prepared rutile calcined at 800 °C.
[c] As-prepared brookite calcined at 300 °C.
[d] As-prepared brookite calcined at 450 °C.
[e] As-prepared brookite calcined at 750 °C.
[f] As-prepared brookite calcined at 900 °C.
[g] pH 3.3 was obtained by adjustment with HCl.

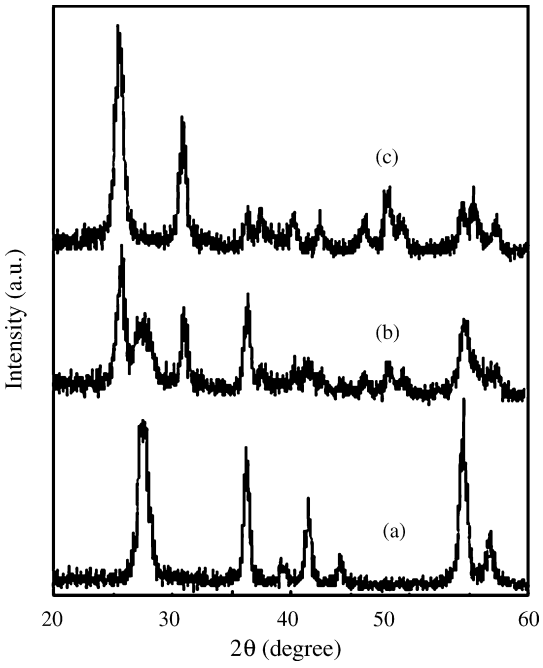

Fig. 4. XRD patterns of the solids obtained by thermolysis of a solution of $TiCl_4$ (0.15 mol dm^{-3}) in diluted HCl ([Cl]/[Ti] = 26) under reflux for 48 h. (a) Rutile; (b) mixture of brookite and rutile; (c) brookite.

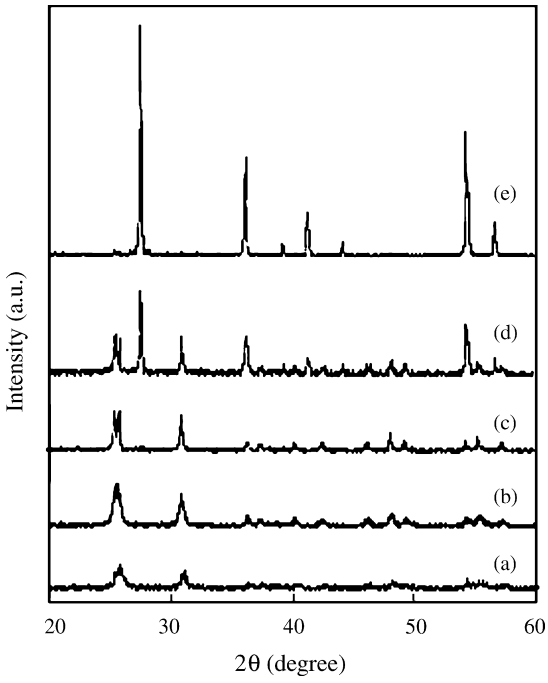

Fig. 6. XRD patterns of brookite particles after heat treatment at different temperatures for 2 h. (a) Sample separated after selective peptization; (b) sample heated at 450 °C; (c) sample heated at 750 °C; (d) sample heated at 800 °C; (e) sample heated at 900 °C.

to 790 °C followed by a small event limited in the 815–845 °C range. The DTG curve highlighted that two overlapping losses, centered at 126 and 287 °C characterized the first intense mass loss (relative intensity of 0.7 and 3.3%, respectively), whereas, the subsequent less intense loss (<0.3%) was strictly confined around 831 °C. Mass spectra of the evolved gas, recorded in the 75–790 °C interval, revealed the release of water and HCl. The trend of the DTA curve was less meaningful showing a very broad endothermic band during the main mass loss. Nevertheless, a small exothermic band centered at 831 °C, was detected with respect to the signal drift according to the DTG sharp peak that should be related to the crystalline phase transformation from brookite to rutile. Calcination up to 1000 °C led to the complete conversion of the solid.

Only rutile formed when the hydrolysis of $TiCl_4$ occurred in the presence of concentrated HCl, whereas mixtures of anatase, brookite and rutile were always obtained from NaCl solutions (see Table 1). Fig. 8 shows the XRD patterns of ternary TiO_2 mixtures formed in the presence of various amounts of NaCl. For $[TiCl_4] = 0.22$ mol dm^{-3}, the increase of the Cl^- concentration gave rise to an increase of the relative amount of rutile (Fig. 8a and b) and a decrease of the percentage of anatase. On the other hand, for $[TiCl_4] = 0.09$ mol dm^{-3} (Fig. 8c), the higher pH value due to a lower amount of HCl produced by the hydrolysis of $TiCl_4$, favored the formation of anatase in spite of the presence of a high [Cl]/[Ti] molar ratio.

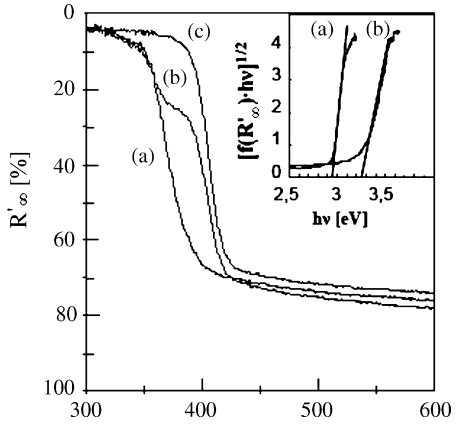

Fig. 5. Diffuse reflectance spectra of the solids obtained by thermolysis of a solution of $TiCl_4$ (0.15 mol dm^{-3}) in diluted HCl ([Cl]/[Ti] = 26) under reflux for 48 h. (a) Brookite; (b) mixture of brookite and rutile; (c) rutile. Inset: plot of the square root of the modified Kubelka-Munck function vs. the energy of the absorbed light. (a) Rutile; (b) brookite.

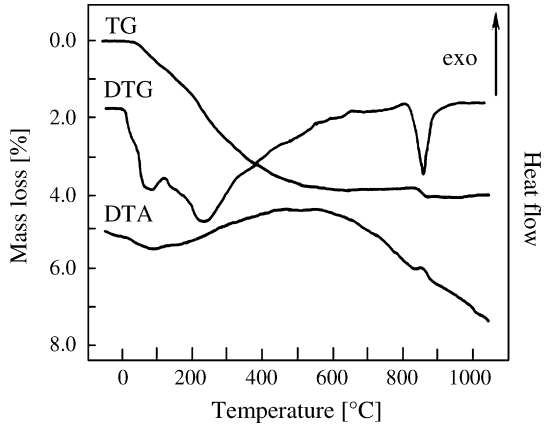

Fig. 7. Thermal analysis of pure brookite sample, heating rate of 10 °C min^{-1} under He flow.

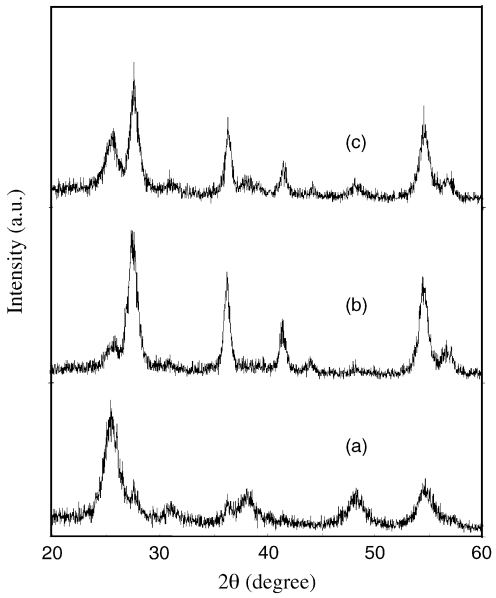

Fig. 8. XRD patterns of the solids obtained by thermolysis of $TiCl_4$ in NaCl solutions at 100 °C in the oven for 48 h. (a) $[TiCl_4] = 0.22\ mol\ dm^{-3}$, [Cl]/[Ti] = 18; (b) $[TiCl_4] = 0.22\ mol\ dm^{-3}$, [Cl]/[Ti] = 26; (c) $[TiCl_4] = 0.09\ mol\ dm^{-3}$, [Cl]/[Ti] = 38.

Data evaluated from the physisorption measurements are reported in Table 2. The rutile samples, obtained in diluted or concentrated HCl, showed specific surface area values higher than that of the commercial rutile powder (Tioxide). Moreover, type IIa isotherms [37] were detected for the as-prepared samples, whereas type I isotherm was found for the commercial specimen. The pure brookite samples displayed again type IIa isotherms that were irrespective of the calcination temperature; on the other hand, a progressive decrease in SSA values was determined as a function of the increasing temperature. The binary and ternary mixtures of the TiO_2 polymorphs showed a more complex trend: both type II and IV isotherms were detected, indicating the existence of macro- and meso-porosities. The surface areas of the mixtures were quite high and decreased with increasing the percentage of rutile.

3.2. Photoreactivity results

The disappearance of 4-NP was followed by determining the concentration of the substrate at various time intervals. The photoactivity of the various powders was compared with that of commercial Degussa P25 TiO_2. The degradation rate, r_o, was calculated from the initial slope of the concentration versus time profiles. r_o values are reported in Table 2.

All the powders obtained by thermolysis of $TiCl_4$ were active for the photodegradation of 4-NP. The photocatalytic activity of the samples, as well their composition, depended on the preparation route. The powders of rutile exhibited a slight photoactivity, differently from the commercial rutile sample, which was practically inactive. The activity of rutile was higher when the powders were obtained in concentrated HCl solutions but decreased if the sample was calcined at 800 °C.

Pure brookite revealed a good photocatalytic activity. The efficiency of the samples increased with increasing temperature, reached a maximum and then decreased for temperatures higher than 750 °C. The highest r_o values were generally obtained with powders consisting of more than one crystalline phase. The samples containing anatase, brookite and rutile were more active than those consisting only of brookite and rutile, while the efficiency of the powders decreased with increasing the percentage of rutile.

4. Discussion

The physical properties of the products obtained by the sol–gel method are strongly influenced by the synthetic variables. Acidity, titanium concentration and temperature govern morphology, size and structure of the TiO_2 nanoparticles synthesized by thermohydrolysis of $TiCl_4$. In particular, the nature of the counterions is determinant for the nature of the crystalline phases. The presence of HCl [11] or HNO_3 [14] in specific domains of acidity allows to obtain the phase brookite.

The experimental results indicated that the relative proportions of the TiO_2 polymorphic phases obtained by thermolysis of $TiCl_4$ in aqueous chloride solutions depend on the pH and the total concentration of HCl in the precipitation solution [11–13]. These two decisive factors are determined by the amounts of $TiCl_4$ and of HCl eventually added. The formation of the different TiO_2 structures can be related to the existence of octahedral hydroxochloro complexes of the type $[Ti(OH)_aCl_b(OH_2)_c]^{(4-a-b)+}$ where $a+b+c=6$, and a and b depend on the acidity and the concentration of Cl^- in the solution [11,38]. The precipitation of solid occurs when, as a consequence of thermolytic or hydrothermic treatments, a neutral complex forms by elimination of hydroxo or chloride ligands [11]. The octahedra link together by olation, through dehydration reactions between aquo and hydroxo ligands forming different structures of polymers by sharing equatorial or apical edges. Further growth proceeds by oxolation with HCl elimination and formation of oxo bridges among the octahedra.

According to Pottier et al. [11], the precursors of rutile and brookite are $[Ti(OH)Cl_3(OH_2)_2]^0$ and $[Ti(OH)_2Cl_2(OH_2)_2]^0$, respectively. When the acidity is high, the solution prevalently contains a large amount of $[Ti(OH)Cl_3(OH_2)_2]^0$ complexes. As shown in Fig. 9a, the $[Ti(OH)Cl_3(OH_2)_2]^0$ monomers can combine by olation only by sharing equatorial edges. In this case, only rutile crystallites are developed. Further condensation involves obviously the substitution of chloride ions with OH ligands.

In diluted HCl solutions, the $[Ti(OH)_2Cl_2(OH_2)_2]^0$ monomers can form skewed chains sharing apical edges (Fig. 9b) so that both anatase and brookite crystallites can be obtained contemporaneously. With increasing time of thermolysis, the pH of the solution decreases [12] and the anatase crystallites transform to brookite and rutile that are the phases more stable in the presence of high amounts of H^+ and Cl^- ions. When the [Cl]/[Ti] molar ratio is high the probability to find hydroxochloro complexes with three chloride anions

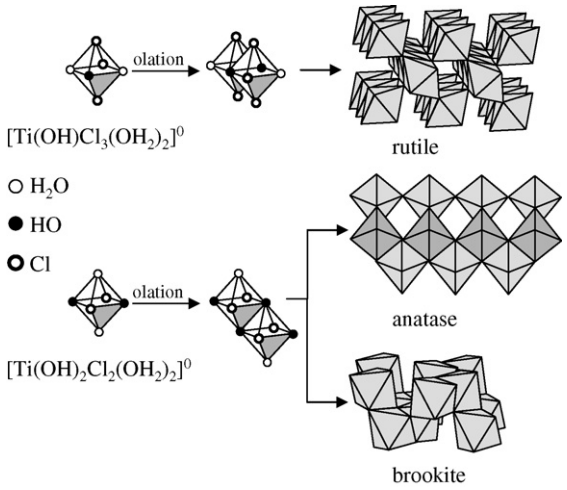

Fig. 9. Possible reaction pathways for the formation of rutile, anatase or brookite starting from octahedral complexes $[Ti(OH)Cl_3(OH_2)_2]^0$ and $[Ti(OH)_2Cl_2(OH_2)_2]^0$.

in the coordination sphere is larger, which should favor the formation of rutile.

In NaCl solutions, the relative proportion of brookite in the mixtures of the three phases is low suggesting that the presence of a large amount of $[Ti(OH)_2Cl_2(OH_2)_2]^0$ monomers is necessary for the formation of brookite. Nabivanets et al. [39] reported that at high Cl^- concentration and low H^+ concentration, complexes containing the tytanil ion TiO^{2+} predominate in solution so that a different condensation pathway could favor the formation of anatase.

As-precipitated rutile powders showed typical type II isotherms, indicating a non-porous matrix, in agreement with data reported for titanium dioxide powders [37]. On the other hand, calcined rutile powders displayed type I isotherms, due to the presence of micropores. These data can be explained with the presence of a large number of inaccessible sites on the powder surface due to the presence of adsorbed water and/or hydroxyls groups bonded to titanium atoms [37]. Pure brookite samples did not show surface features far from the rutile powders: again non-porous systems were revealed from the physisorption measurements, with a progressive decrease in surface area values with increasing the treatment temperature. On the other hand, the mass spectra data recorded during the thermogravimetric analysis of the brookite sample indicated that the as-prepared powders showed a continuous release of water during the heating treatment. The endothermic H_2O evolution arose from simply desorption of adsorbed molecules at lower temperatures and then from the condensation of residual surface ≡Ti–OH groups. This thermal activated condensation led to a progressive decrease of the specific surface area values and to an increase of the crystallite mean dimensions of the residual solid, as shown in Table 2.

The thermohydrolysis of $TiCl_4$ in aqueous chloride solutions did not allow to obtain directly pure brookite but only binary or ternary mixtures of the three TiO_2 polymorphs. The separation of the brookite particles from mixtures of brookite and rutile has been previously carried out by peptization with nitric acid [11]. To avoid that the presence of NO_3^- could influence the photocatalytic properties of the powders, the selective peptization of brookite was obtained more simply by diluting many times the mixture of brookite and rutile and separating the supernatant dispersion from the solid. The difference in peptizability of the two types of particles is due to the different sizes of the aggregates of brookite and rutile. The aggregates of rutile consisted of heavier and bigger particles as confirmed by the lower value of specific surface area (see Table 2), although the crystallite sizes were often smaller than those of brookite. As a result, type IV isotherms, attributable to mesoporous systems, were found for these samples. The powders obtained from both diluted HCl and NaCl solutions displayed a more reactive surface and the corresponding surface area values decreased with increasing the amount of the rutile polymorph.

The diffuse reflectance measurements have allowed to determine the band gap of bulky brookite. The value of 3.29 eV determined for the powder calcined at 450 °C is in good agreement with the few data reported in literature. Grätzel and Rotzinger [35] estimated the E_g value of brookite as 3.14 eV by extended Hückel MO calculations. Koelsch et al. [21] determined the band gap of brookite nanoparticles as 3.4 eV, measuring the optical transmission of brookite dispersions at different concentrations and by UV fluorescence measurements. Shibata et al. [36] photoelectrochemically determined a band gap value of 3.26 eV for films consisting mostly of brookite phase with some anatase.

XRD analysis showed that by calcination at high temperatures, brookite transformed directly to rutile, without the involvement of the anatase polymorph. This finding agrees with the results of previous works that report a direct brookite–rutile transition [5,14,18,32,40] although some authors claim that brookite transforms to rutile via anatase [19,41,42].

The transformation sequence among anatase, brookite and rutile depends on several factors including crystallite size, size distribution and contact area of the crystallites in the powder. Zhang and Banfield found a correlation among the surface enthalpies of the three polymorphs and their particle size [40]. The energies of anatase, brookite and rutile are sufficiently close that they can be reversed by small differences in surface energies. Brookite is more stable than anatase for crystal sizes greater than 11 nm while rutile is the most stable phase at sizes greater than 35 nm [40]. Similar results were obtained through free energies calculations [43]. Anatase is the most stable phase when the size is smaller than 4.9 nm, brookite for sizes between 4.9 and 30 nm, and rutile for sizes larger than 30 nm. Zhu et al. [43] developed an empirical expression on a critical grain size of brookite, D_c, which dominates the transition sequence between anatase and brookite. When the size of brookite D_b is larger than D_c, brookite directly transforms to rutile whereas, when D_b is smaller than D_c, brookite transforms to anatase and then anatase to rutile.

As shown in Table 2, our as-prepared brookite had a crystallite size of 6.6 nm and a specific surface area of 82 $m^2\,g^{-1}$. By heating at increasing temperatures the size progressively grew enhancing the stability of the brookite phase. At temperature higher than 750 °C the crystallite size probably reached a criti-

cal value and brookite directly transformed to rutile. The perusal of the DTA curve indicates that the transformation of brookite occurred in the temperature range 815–845 °C.

The photocatalytic activity of TiO_2 is one of its technologically most attractive properties. The reactivity of the TiO_2 nanoparticles depends on several factors including specific surface area, crystallinity, crystallite size and crystal structure. The reduced size of the particles leads to larger surface areas, and consequently the number of available surface active sizes increases. A reduction in particle size should also lead to a high photonic efficiency favoring a higher interfacial charge carrier transfer rate.

The photoactivity of the powders, as well as their composition, depend on the preparation route. All rutile samples synthesized by thermolysis of $TiCl_4$ in HCl solutions degraded 4-nitrophenol under UV irradiation differently from commercial rutile Tioxide, whose activity was negligible. This probably depends on the particular physicochemical features of the nanostructured powders as, for instance, a larger extent of surface hydroxylation. By thermal treatment at 800 °C the activity of rutile decreased due to the noticeable reduction of its specific surface area.

Pure brookite samples revealed good photocatalytic activity in spite of the high value of E_g and the poor crystalline phase. The enhancement of efficiency obtained by calcination at 450 °C is attributable to the improved cristallinity of the powder. The low photoactivity exhibited by the sample calcined at 900 °C is ascribable both to the phase transformation to rutile and the drastic decrease in specific surface area.

Previous reports indicated that brookite may be used as an effective photocatalyst. Brookite nanocrystals synthesized by air oxidation of $TiCl_3$ in aqueous HCl solution, were more photoactive than anatase Merck for both the reactions of H_2 formation from 2-propanol and O_2 evolution from Ag_2SO_4 solutions [16]. Rates of CO_2 or H_2 formation comparable to those of Degussa P25 were exhibited by some brookite samples, prepared by solvothermal treatment of oxobis(2,4-pentanedionato-O,O′)titanium [6,7] and tested for the mineralization of CH_3COOH and dehydrogenation of 2-propanol, respectively. Pure brookite nanocrystals obtained by reaction of a mixed solution of urea and $TiCl_3$ showed good photocatalytic properties for the degradation of acetaldehyde [17] and 4-chlorophenol [19] but the activity of these samples was rather lower than that of Degussa P25. Moreover, Koelsch et al. [21] found that brookite is more electrochemically active than anatase and is a good candidate for photovoltaic devices. Very recent studies have demonstrated that the brookite structure is stable for reversible lithium intercalation and deintercalation and that there are no major structural changes in contrast to the Li intercalation into rutile [44].

The photoactivity of Degussa P25 for the degradation of 4-nitrophenol is still higher than that of the brookite powders obtained by thermolysis of $TiCl_4$ in diluted HCl solutions. Anyway, thin films prepared by dip coating from the water dispersion containing only brookite particles were more active than films of anatase and rutile for the photodegradation of 2-propanol in gas–solid regime [23].

Table 2 shows that the highest r_o values were obtained with samples consisting of more than one crystalline phase. The contemporaneous presence of different phases of the same semiconductor is usually beneficial to enhance the photocatalytic activity [27,45–51] and in particular, the very active commercial Degussa P25 is composed of anatase and rutile. Ozawa et al. [46] attributed the high photoactivity exhibited by anatase–brookite composite nanocrystals to the junction between anatase and brookite. As already demonstrated for other systems [47–49] the coupling of different semiconductors allows the vectorial displacement of holes and electrons from one semiconductor to another and retards the recombination of the electron/hole pairs. Yu et al. [50,51] reported that the photoactivity of powders containing 80% anatase and 20% brookite exceeded that of Degussa P25 for the oxidation of propanone in air.

The powders obtained by thermolysis of $TiCl_4$ in aqueous NaCl solutions consisted of anatase, brookite and rutile and were more active than those containing only brookite and rutile obtained in HCl solutions. The band gap values of the ternary or binary mixtures were lower than those of pure anatase or brookite. These findings are in accord with the results of Lopez et al. [27] who found that the highest photoactivity among TiO_2 sol–gel catalysts tested for the decomposition of 2,4-dinitroaniline corresponded to the sample having the lowest E_g and composed of anatase, brookite and rutile.

5. Conclusion

The reaction time as well as the final concentration of HCl were the decisive factors in determining the composition of the TiO_2 powders synthesized by thermohydrolysis of $TiCl_4$ in aqueous chloride solutions. Nanocrystalline rutile was obtained both in concentrated and diluted HCl. Mixtures of brookite and rutile precipitated in diluted HCl depending on the acidity of the medium or the titanium concentration. Ternary mixtures of anatase, brookite and rutile were always formed in NaCl solutions.

Stable sols of pure brookite were easily peptized from mixtures of brookite and rutile obtained from mild acidic solutions without addition of HNO_3 but only by dilution. Direct phase transformation from brookite to rutile occurred with heating.

The brookite particles revealed good catalytic properties for the photodegradation of 4-nitrophenol. The powder calcined at 450 °C exhibited a higher reactivity, mainly because of its increased crystallinity. The highest photocatalytic activity corresponded to the samples in which anatase, brookite and rutile coexisted.

References

[1] A. Fujishima, K. Hashimoto, T. Watanabe, TiO_2 Photocatalysis: Fundamentals and Applications, Bkc, Tokyo, 1999.
[2] I. Keesmann, Zur hydrothermalen Synthese von Brookit, Z. Anorg. Allg. Chem. 346 (1966) 30–43.
[3] T. Mitsuhashi, M. Watanabe, Brookite formation from precipitates containing calcium ions, Miner. J. 9 (1978) 236–240.
[4] T. Nagase, T. Ebina, T. Iwasaki, H. Hayashi, Y. Onodera, M. Chatterjee, Hydrothermal synthesis of brookite, Chem. Lett. (1999) 911–912.

[5] H. Kominami, M. Kohno, Y. Kera, Synthesis of brookite-type titanium oxide nano-crystals in organic media, J. Mater. Chem. 10 (2000) 1151–1156.
[6] H. Kominami, J.-I. Kato, S.-Y. Murakami, Y. Ishii, M. Kohno, K.-I. Yabutani, T. Yamamoto, Y. Kera, M. Inoe, T. Inui, B. Ohtani, Solvothermal syntheses of semiconductor photocatalysts of ultra-high activities, Catal. Today 84 (2003) 181–189.
[7] H. Kominami, Y. Ishii, M. Kohno, S. Konishi, Y. Kera, B. Ohtani, Nanocrystalline brookite-type titanium(IV) oxide photocatalysts prepared by a solvothermal method: correlation between their physical properties and photocatalytic activities, Catal. Lett. 91 (2003) 41–47.
[8] Y. Zheng, E. Shi, S. Cui, W. Li, X. Hu, Hydrothermal preparation and characterization of brookite-type TiO_2 nanocrystallites, J. Mater. Sci. Lett. 19 (2000) 1445–1448.
[9] W. Luo, S.F. Yang, Z.C. Wang, R. Ahuja, B. Johansson, J. Liu, G.T. Zou, Structural phase transitions in brookite-type TiO_2 under high pressure, Solid State Commun. 133 (2005) 49–53.
[10] K. Tomita, V. Petrykin, M. Kobayashi, M. Shiro, M. Yoshimura, M. Kakihana, A water-soluble titanium complex for the selective synthesis of nanocrystalline brookite, rutile, and anatase by a hydrothermal method, Angew. Chem. Int. Ed. 45 (2006) 2378–2381.
[11] A. Pottier, C. Chanéac, E. Tronc, L. Mazerolles, J.P. Jolivet, Synthesis of brookite TiO_2 nanoparticles by thermolysis of $TiCl_4$ in strongly acidic aqueous media, J. Mater. Chem. 11 (2001) 1116–1121.
[12] J.H. Lee, Y.S. Yang, Effect of HCl concentration and reaction time on the change in the crystalline state of TiO_2 prepared from aqueous $TiCl_4$ solution by precipitation, J. Eur. Ceram. Soc. 25 (2005) 3573–3578.
[13] J.H. Lee, Y.S. Yang, Effect of hydrolysis conditions on morphology and phase content in the crystalline TiO_2 nanoparticles synthesized from aqueous $TiCl_4$ solution by precipitation, Mater. Chem. Phys. 93 (2005) 237–242.
[14] J.H. Lee, Y.S. Yang, Synthesis of TiO_2 nanoparticles with pure brookite at low temperature by hydrolysis of $TiCl_4$ using HNO_3 solution, J. Mater. Sci. 41 (2006) 557–559.
[15] B.I. Lee, X. Wang, R. Bhave, M. Hu, Synthesis of brookite TiO_2 nanoparticles by ambient condition sol process, Mater. Lett. 60 (2006) 1179–1183.
[16] B. Ohtani, J.-I. Handa, S.-I. Nishimoto, T. Kagiya, Highly active semiconductor photocatalyst: Extra-fine crystallite of brookite TiO_2 for redox reaction in aqueous propan-2-ol and/or silver sulfate solution, Chem. Phys. Lett. 120 (1985) 292–294.
[17] J.-G. Li, C. Tang, D. Li, H. Haneda, T. Ishigaki, Monodispersed spherical particles of brookite-type TiO_2: synthesis, characterization, and photocatalytic property, J. Am. Ceram. Soc. 87 (2004) 1358–1361.
[18] J.-G. Li, T. Ishigaki, Brookite → rutile phase transformation of TiO_2 studied with monodispersed particles, Acta Mater. 52 (2004) 5143–5150.
[19] S. Bakardjieva, V. Stengl, L. Szatmary, J. Subrt, J. Lukac, N. Murafa, D. Niznansky, K. Cizek, J. Jrkovsky, N. Petrova, Transformation of brookite-type TiO_2 nanocrystals to rutile: correlation between microstructure and photoactivity, J. Mater. Chem. 16 (2006) 1709–1716.
[20] S.-J. Kim, K. Lee, J.H. Kim, N.-L. Lee, S.-J. Kim, Preparation of brookite phase TiO_2 colloidal sol for thin film coating, Mater. Lett. 60 (2006) 364–367.
[21] M. Koelsch, S. Cassaignon, J.F. Guillemoles, J.-P. Jolivet, Comparison of optical and electrochemical properties of anatase and brookite TiO_2 synthesized by the sol–gel method, Thin Solid Films 403–404 (2002) 312–319.
[22] A. Di Paola, M. Addamo, M. Bellardita, E. Cazzanelli, L. Palmisano, Preparation of photocatalytic brookite thin films, Thin Solid Films 515 (2007) 3527–3529.
[23] M. Addamo, M. Bellardita, A. Di Paola, L. Palmisano, Preparation and photoactivity of nanostructured anatase, rutile and brookite TiO_2 thin films, Chem. Commun. (2006) 4943.
[24] I.N. Kuznetsova, V. Blaskov, I. Stambolova, L. Znaidi, A. Kanaev, TiO_2 pure phase brookite with preferred orientation, synthesized as a spin-coated film, Mater. Lett. 59 (2005) 3820–3823.
[25] A. Sclafani, L. Palmisano, M. Schiavello, Influence of the preparation methods of titanium dioxide on the photocatalytic degradation of phenol in aqueous dispersion, J. Phys. Chem. 94 (1990) 829–832.
[26] M. Addamo, M. del Arco, M. Bellardita, D. Carriazo, A. Di Paola, E. García-López, G. Marcì, C. Martín, L. Palmisano, V. Rives, Photoactivity of nanostructured TiO_2 catalysts in aqueous system and their surface acid-base, bulk and textural properties, Res. Chem. Intermed. 33 (2007) 46–479.
[27] T. Lopez, R. Gomez, E. Sanchez, F. Tzompantzi, L. Vera, Photocatalytic activity in the 2,4-dinitroaniline decomposition over TiO_2 sol–gel derived catalysts, J. Sol–gel Sci. Technol. 22 (2001) 99–107.
[28] S.D. Park, Y.H. Cho, W.W. Kim, S.-J. Kim, Understanding of homogeneous spontaneous precipitation for monodispersed TiO_2 ultrafine powders with rutile phase around room temperature, J. Solid State Chem. 146 (1999) 230–238.
[29] S. Dirè, R. Ceccato, F. Babonneau, Structural and microstructural evolution during pyrolysis of hybrid polydimethylsiloxane-titania nanocomposites, J. Sol–Gel Sci. Technol. 34 (2005) 53–62.
[30] B.E. Warren, B.L. Averbach, The effect of cold-work distortion on X-ray patterns, J. Appl. Phys. 21 (1950) 595–599.
[31] R. Campostrini, G. D'Andrea, G. Carturan, R. Ceccato, G.D. Sorarù, Pyrolysis study of methyl-substituted Si—H containing gels as precursors for oxycarbide glasses, by combined thermogravimetry, gas chromatographic and mass spectrometric analysis, J. Mater. Chem. 6 (1996) 585–594.
[32] X. Bokhimi, F. Pedraza, Characterization of brookite and a new corundum-like titania phase synthesized under hydrothermal conditions, J. Solid State Chem. 177 (2004) 2456–2463.
[33] F.P. Koffyberg, K. Dwight, A. Wold, Interband transitions of semiconducting oxides determined from photoelectrolysis spectra, Solid State Commun. 30 (1979) 433–437.
[34] Y.I. Kim, S.J. Atherton, E.S. Brigham, T.E. Mallouk, Sensitized layered metal oxide semiconductor particles for photochemical hydrogen evolution from nonsacrificial electron donors, J. Phys. Chem. 97 (1993) 11802–11810.
[35] M. Grätzel, F.P. Rotzinger, The influence of the crystal lattice structure on the conduction band energy of oxides of titanium(IV), Chem. Phys. Lett. 118 (1985) 474–477.
[36] T. Shibata, H. Irie, M. Ohmori, A. Nakajima, T. Watanabe, K. Hashimoto, Comparison of photochemical properties of brookite and anatase TiO_2 films, Phys. Chem. Chem. Phys. 6 (2004) 1359–1362.
[37] F. Rouquerol, J. Rouquerol, K. Singh, Adsorption by Powders and Porous Solids, Academic Press, San Diego, 1999.
[38] H. Cheng, J. Ma, Z. Zhao, L. Qi, Hydrothermal preparation of uniform nanosize rutile and anatase particles, Chem. Mater. 7 (1995) 663–671.
[39] B.I. Nabivanets, L.N. Kudritskaya, A study of the polymerisation of titanium(IV) in hydrochloric acid solutions, Russ. J. Inorg. Chem. 12 (1967) 616–620.
[40] H. Zhang, J.F. Banfield, Understanding polymorphic phase transformation behavior during growth of nanocrystalline aggregates: insights from TiO_2, J. Phys. Chem. B 104 (2000) 3481–3487.
[41] X. Ye, J. Sha, Z. Jiao, L. Zhang, Thermoanalytical characteristic of nanocrystalline brookite-based titanium dioxide, Nanostruct. Mater. 8 (1997) 919–927.
[42] W.W. So, S.B. Park, K.J. Kim, C.H. Shin, S.J. Moon, The crystalline phase stability of titania particles prepared at room temperature by the sol–gel method, J. Mater. Sci. 36 (2001) 4299–4305.
[43] K.-R. Zhu, M.-S. Zhang, J.-M. Hong, Z. Yin, Size effect on phase transition sequence of TiO_2 nanocrystal, Mater. Sci. Eng. A 403 (2003) 87–93.
[44] M.A. Reddy, M.S. Kishore, V. Pralong, U.V. Varadaraju, B. Raveau, Lithium intercalation into nanocrystalline brookite TiO_2, Electrochem. Solid-State Lett. 10 (2007) A29–A31.
[45] R.I. Bickley, T. Gonzales-Carreno, J.S. Lees, L. Palmisano, R.J.D. Tilley, A structural investigation of titanium dioxide photocatalysts, J. Solid State Chem. 92 (1991) 178–190.
[46] T. Ozawa, M. Iwasaki, H. Tada, T. Akita, K. Tanaka, S. Ito, Low-temperature synthesis of anatase–brookite composite nanocrystals: the junction effect on photocatalytic activity, J. Colloid Interface Sci. 281 (2005) 510–513.
[47] S. Hotchandani, P.V. Kamat, Charge-transfer processes in coupled semiconductor systems. Photochemistry and photoelectrochemistry of the colloidal cadmium sulfide-zinc oxide system, J. Phys. Chem. 96 (1992) 6834–6839.
[48] N. Serpone, P. Maruthamuthu, P. Pichat, E. Pelizzetti, H. Hidaka, Exploiting the interparticle electron transfer process in the photocatalysed oxidation

of phenol, 2-chlorophenol and pentachlorophenol: chemical evidence for electron and hole transfer between coupled semiconductors, J. Photochem. Photobiol. A: Chem. 85 (1995) 247–255.

[49] A. Di Paola, L. Palmisano, M. Derrigo, V. Augugliaro, Preparation and characterization of tungsten chalcogenide photocatalysts, J. Phys. Chem. B 101 (1997) 876–883.

[50] J.C. Yu, J. Yu, L. Zhang, W. Ho, Enhancing effects of water content and ultrasonic irradiation on the photocatalytic activity of nano-sized TiO_2 powders, J. Photochem. Photobiol. A: Chem. 148 (2002) 263–271.

[51] J. Yu, J.C. Yu, M.K.-P. Leung, W. Ho, B. Cheng, X. Zhao, J. Zhao, Effects of acidic and basic hydrolysis catalysts on the photocatalytic activity and microstructures of bimodal mesoporous titania, J. Catal. 217 (2003) 69–78.